Available online at www.sciencedirect.com
ScienceDirect
Proceedings of the Combustion Institute 000 (2016) 1–8
Proceedings of the Combustion Institute
www.elsevier.com/locate/proci

An analytical model for the impulse response of laminar premixed flames to equivalence ratio perturbations

A. Albayrak, R.S. Blumenthal, A. Ulhaq, W. Polifke*

Professur für Thermofluiddynamik, Technische Universität München, Boltzmannstr. 15, Garching D-85748, Germany

Received 2 December 2015; accepted 1 June 2016
Available online xxx

Abstract

The dynamic response of conical laminar premixed flames to fluctuations of equivalence ratio is analyzed in the time domain, making use of a level set method ("*G*-Equation"). Perturbations of equivalence ratio imposed at the flame base are convected towards the flame front, where they cause modulations of flame speed, heat of reaction and flame shape. The resulting fluctuations of heat release rate are represented in closed form in terms of respective impulse response functions. The time scales corresponding to these mechanisms are identified, their contributions to the overall flame impulse response are discussed. If the impulse response functions are Laplace transformed to the frequency domain, agreement with previous results for the flame frequency response is observed. An extension of the model that accounts for dispersion of equivalence ratio fluctuations due to molecular diffusion is proposed. The dispersive model reveals the sensitivity of the premixed flame dynamics to the distance between the flame and the fuel injector. The model results are compared against numerical simulation of a laminar premixed flame.

Keywords: Laminar premixed flame dynamics; Equivalence ratio perturbation; Impulse response; Flame frequency response; Dispersion

1. Introduction

Modern low-emission combustion processes often utilize premixed combustion with lean fuel-air mixtures. However, premixed combustion is prone to thermo-acoustic instabilities, where positive feedback between fluctuating heat release and acoustics drives self-excited oscillations. Large amplitude oscillations can cause damage to a combustor, thus it is necessary to understand the physics of lean premixed combustion dynamics and reveal key factors and interaction mechanisms responsible for instabilities.

Premixed flame dynamics is driven mainly by velocity and equivalence ratio perturbations. The corresponding interaction mechanisms have been studied extensively by means of analytical models, numerical simulations and experiments, as described by Lieuwen [1]. First analytical studies of the dynamic response of anchored premixed flames to velocity perturbation were carried out by Boyer and Quinard [2] and Fleifil et al. [3]. Schuller

* Corresponding author.
E-mail address: polifke@tfd.mw.tum.de (W. Polifke).

http://dx.doi.org/10.1016/j.proci.2016.06.002
1540-7489 © 2016 by The Combustion Institute. Published by Elsevier Inc.

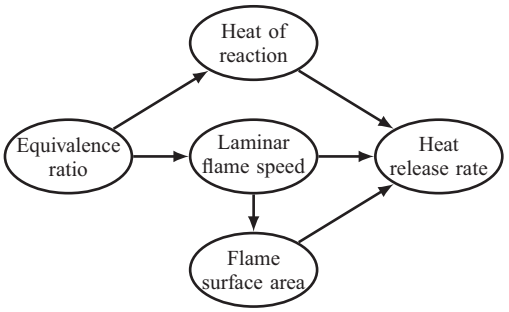

Fig. 1. Major mechanisms contributing to heat release rate oscillations [7].

et al. [4] presented a comprehensive treatment for various flame shapes, and compared analytical results against numerical and experimental data. All these studies were based on a linearized version of the so-called *G-Equation*, i.e. a kinematic equation for a propagating flame front [5]. Using the same framework, the response of laminar premixed flames to equivalence ratio perturbations was studied by Dowling and Hubbard [6] and by Lieuwen and co-authors [7–9].

The conventional way of representing the flame response to both velocity and equivalence ratio perturbations relies on the *Flame Transfer Functions* (FTF) in the frequency domain. Such a frequency domain approach is very convenient for asymptotic stability analysis, but poses a challenge for the physics-based interpretation of transient flow–flame interactions. A time domain approach, based on the *Impulse Response* (IR) function, appears more suitable for this purpose, even though fundamentally FTF and IR contain the same information. The IR of premixed flames to velocity perturbations was determined by Blumenthal et al. [10] using the linearized *G*-Equation. The time domain perspective allowed straightforward identification of characteristic time scales and gave additional insight into the pertinent flow–flame interactions. Moreover, complete correspondence with frequency domain results by Schuller et al. [4] could be established.

In the present work, the impulse response of a conical premix flame to perturbations of equivalence ratio is derived analytically. Following Lieuwen and co-workers [7–9], the dominant interaction mechanisms between fluctuations of equivalence ratio and heat release rate are considered (see Fig. 1): Firstly, perturbations in equivalence ratio modulate the heat of reaction and the laminar flame speed, which affect the heat release rate of the flame in a direct manner [11,12]. Moreover, changes in laminar flame speed disturb the kinematic balance between flow and flame, such that the flame shape and the flame surface area are also perturbed. This is an indirect, but important effect, first discussed by Lawn and Polifke [11]. Other contributions, i.e. flame stretch and curvature, gas expansion, flame confinement and anchoring, are not considered in the present analysis.

Like earlier studies [2–4,7–9], the present work uses the linearized *G*-Equation, but in the time domain. More insight into the physics of flame dynamics is expected to result from such a treatment. It will be confirmed that the overall flame dynamics can be described by the superposition of the mechanisms depicted in Fig. 1. The respective contributions to the overall flame response are determined by individual IRs and relevant time scales are identified. Furthermore, an extension of the model is proposed, which considers the effect of dispersion on the spatio-temporal distribution of equivalence ratio perturbations and on the flame dynamics.

The paper is structured as follows: A model for premixed flame dynamics based on the linearized *G*-Equation is described in the next section. Heat release rate fluctuations caused by perturbations of equivalence ratio are described in terms of impulse responses. For each of the contributions depicted in Fig. 1, the respective IR is derived and explained in Section 3. Eventually the flame transfer functions of Shreekrishna et al. [8] are recovered. In Section 4, the dispersive model is introduced. Results of a validation study against numerical simulation is presented in Section 5.

2. Modeling tools

2.1. Modeling of heat release rate fluctuations

Flame dynamics can be investigated with the relation $q(t) = \int_f \rho \Delta H s_L \, \mathrm{d}A$ for the unsteady heat release rate of a premixed flame in linearized form

$$\frac{q'(t)}{\bar{q}} = \int_f \frac{\Delta H'}{\Delta \bar{H}} \frac{\mathrm{d}A}{\bar{A}} + \int_f \frac{s'_L}{\bar{s}_L} \frac{\mathrm{d}A}{\bar{A}} + \frac{A'(t)}{\bar{A}} , \qquad (1)$$

where $\bar{(\,)}$ and $(\,)'$ stand for the steady and fluctuating quantities, respectively. ΔH is the heat of reaction, s_L is the laminar flame speed and A is the flame surface area. The fluctuating quantities depend on the local values of equivalence ratio ϕ. The unburnt gas density ρ is assumed to be constant. The major contributions to heat release rate fluctuations discussed above (see Fig. 1) appear explicitly on the r.h.s. of the equation.

2.2. G-Equation approach for flame shape

The flame surface motion is modeled with the *G-Equation*, i.e. a level set approach that reads

$$\frac{\partial G}{\partial t} + \vec{v} \cdot \vec{\nabla} G = s_L |\vec{\nabla} G|. \qquad (2)$$

Here $\vec{v}$ is the flow velocity and G is the level set function with the flame position at $G = 0$. The

Please cite this article as: A. Albayrak et al., An analytical model for the impulse response of laminar premixed flames to equivalence ratio perturbations, Proceedings of the Combustion Institute (2016), http://dx.doi.org/10.1016/j.proci.2016.06.002

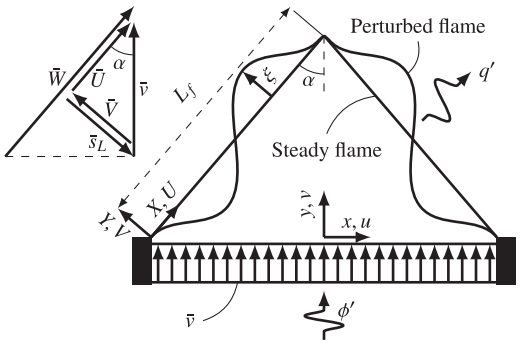

Fig. 2. Flame configuration, important velocities and laboratory (x, y) and flame aligned (X, Y) coordinate systems.

linearized G-Equation can be solved analytically for uniform mean velocity $\vec{v} = (0, \bar{v})$, see Fig. 2. The assumption of linearity limits any perturbations to small amplitudes in order to have an amplitude independent flame response. The flame aligned coordinate system "(X, Y)" is employed instead of the laboratory coordinate system "(x, y)", see Fig. 2. The flame surface motion is assumed to be strictly normal to the flame, mathematically $G(X, Y, t) = Y - \xi(X, t)$. Substituting the perturbation in flame surface position $\xi(X, t)$ in the linearized G-Equation leads to

$$\frac{\partial \xi}{\partial t} + \bar{U}\frac{\partial \xi}{\partial X} = V' - s'_L \,. \tag{3}$$

The velocities U, V and s_L are illustrated in Fig. 2. The flame is assumed to be attached to the wall corners, i.e., $\xi(0, t) = 0$ is used as boundary condition. The analytical solution of Eq. (3) will be employed to determine the contribution of flame surface area fluctuations to the heat release rate in Section 3.3.

2.3. Impulse response (IR) for identification

A general way to quantify linear fluctuations in heat release rate q' caused by equivalence ratio perturbations ϕ' is the *impulse response* $h(\tau)$, which is defined implicitly via

$$\frac{q'(t)}{\bar{q}} = \frac{1}{\bar{\phi}}\int_0^\infty h(\tau)\phi'(y = 0, t - \tau)\,\mathrm{d}\tau \,. \tag{4}$$

Here the source of ϕ' is located at flame base $y = 0$ without loss of generality. If an impulse perturbation $\phi'(y = 0, t) = \bar{\phi}\varepsilon\delta(t)$ is imposed, where δ is the Dirac delta function and ε the relative strength of the perturbation, then correspondingly $q'(t)/\varepsilon\bar{q} = h(t)$, which is why $h(\tau)$ is called the *impulse response*. The effects that contribute to flame response – see Fig. 1 and Eq. (1) – can be investigated separately,

$$h(t) = h_{\Delta H}(t) + h_{s_L}(t) + h_A(t). \tag{5}$$

The FTF $F(\omega)$ is obtained from the IR by Laplace transformation, $F(s) = \int_0^\infty \mathrm{e}^{-st}h(t)\,\mathrm{d}t$ with $s = -i\omega$.

2.4. Transport of equivalence ratio perturbations

The convective transport of equivalence ratio perturbations may be modeled with the 1-D advection equation as

$$\frac{\partial \phi'}{\partial t} + \bar{v}\frac{\partial \phi'}{\partial y} = 0 \,. \tag{6}$$

The analytical solution for an impulse perturbation imposed at flame base $y = 0$ reads

$$\phi'(x, y, t) = \bar{\phi}\varepsilon\delta\left(t - \frac{y}{\bar{v}}\right) = \bar{\phi}\varepsilon\delta\left(t - \frac{X}{\bar{W}}\right) . \tag{7}$$

Physically interpreted, a sudden change in equivalence ratio at the flame base convects in $y-$direction towards the flame tip with the flow velocity $\bar{v}$. Equation (7) also shows how this effect may be represented in the flame-aligned coordinate system.

3. Contributions to the flame impulse response

3.1. Fluctuations of heat of reaction

The first term on the right hand side of Eq. (1) stands for the contribution of heat of reaction fluctuations to the heat release rate. The fluctuation in heat of reaction $\Delta H'$ caused by the equivalence ratio perturbations ϕ' is approximated by a relation $\Delta H = f(\phi)$ from empirical data (valid for CH_4 [7]). First order Taylor series expansion is employed for fluctuating quantities, $\Delta H' = \mathrm{d}\Delta H/\mathrm{d}\phi|_{\phi=\bar{\phi}}\phi'$.

By integrating $\Delta H'$ over the flame surface, the IR contribution is calculated as

$$\begin{aligned} h_{\Delta H}(t) &= \frac{1}{\varepsilon}\int_f \frac{\Delta H'}{\Delta \bar{H}}\frac{\mathrm{d}A}{\bar{A}} \\ &= \frac{1}{\varepsilon}\frac{\mathrm{d}\Delta H}{\mathrm{d}\phi}\bigg|_{\phi=\bar{\phi}}\frac{1}{\Delta \bar{H}\bar{A}}\int_f \phi'\,\mathrm{d}A \,, \end{aligned} \tag{8}$$

where $\bar{A} = \pi L_f^2 \sin\alpha$ is the steady flame surface area and $\mathrm{d}A = 2\pi(L_f - X)\sin\alpha\,\mathrm{d}X$ is the steady infinitesimal flame surface area for a conical flame. By substituting $\phi' = \bar{\phi}\varepsilon\delta\left(t - X/\bar{W}\right)$ as defined in Section 2.4, the IR is obtained in closed form

$$h_{\Delta H}(t) = \frac{2S_{\Delta H}}{\tau_c^2}\{R(t - \tau_c) - R(t) + \tau_c H(t)\}. \tag{9}$$

where $H(t)$ is the Heaviside function and $R(t)$ is the Ramp function. $S_{\Delta H} = \left(\bar{\phi}/\Delta\bar{H}\right)\mathrm{d}\Delta H/\mathrm{d}\phi|_{\phi=\bar{\phi}}$ is the sensitivity of the heat of reaction to the equivalence ratio. $\tau_c = L_f/\bar{W}$ is a convective time scale, which is defined as the time span for the perturbation to travel from the base of the flame to its tip.

Please cite this article as: A. Albayrak et al., An analytical model for the impulse response of laminar premixed flames to equivalence ratio perturbations, Proceedings of the Combustion Institute (2016), http://dx.doi.org/10.1016/j.proci.2016.06.002

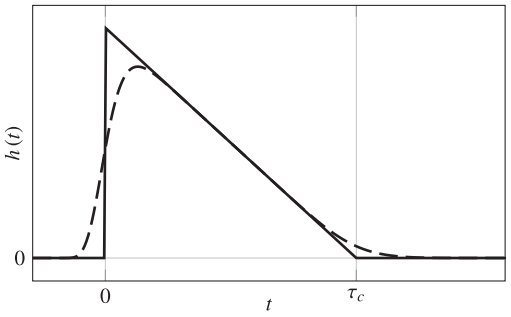

Fig. 3. Contribution of fluctuations in heat of reaction or laminar flame speed to the IR. Models without (——) and with dispersion (– –).

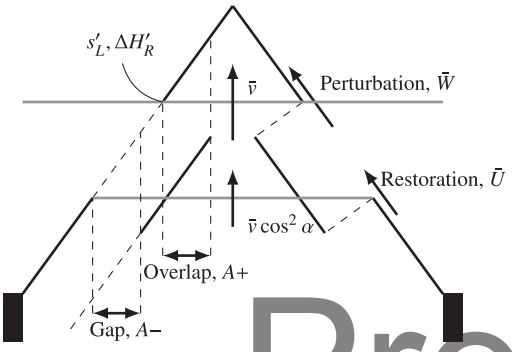

Fig. 4. Intermediate flame shape with relevant velocities for convection of perturbation and restoration process. Visualization of area gap and overlap due to the change in laminar flame speed.

The IR according to Eq. (9) is plotted in Fig. 3 with the solid line.

Laplace Transform as defined in Section 2.3 recovers exactly the analytical expression for the flame transfer function obtained by Shreekrishna et al. [8, Eq. (25)].

For the lean premixed flame, a positive impulse perturbation in the equivalence ratio increases the heat of reaction on the flame surface element located at the instantaneous position of the perturbation. The increase in heat of reaction also increases the heat release rate (see Eq. (1)). In Fig. 4 a flame perturbed by a δ-pulse as defined in Eq. (7) is shown. The upper gray line ("Perturbation, $\bar{W}$") indicates the flame surface element, whose heat of reaction is changed. The incoming perturbation initially acts on the flame at the base, which has the largest radius. As the perturbation is convected towards the flame tip, the resulting perturbation in heat release rate decreases, because the radius of the flame decreases. This fact explains the trend shown in Fig. 3, that the IR contribution is highest at the beginning and decreases until the convective time scale τ_c, when the perturbation reaches the flame tip, which has zero radius.

For rich mixtures, additional fuel barely changes the heat of reaction, which implies that the sensitivity $S_{\Delta H}$ and thus also the corresponding IR are very small.

3.2. Fluctuations of laminar flame speed

The second term on the right hand side of Eq. (1) stands for the contribution of laminar flame speed fluctuations to the heat release rate. The same approach as described in Section 3.1 is employed also for laminar flame speed contribution. The only difference is that $S_{\Delta H}$ is replaced with the sensitivity of laminar flame speed to the equivalence ratio, $S_{s_L} = \left(\bar{\phi}/\bar{s}_L\right) \mathrm{d}s_L/\mathrm{d}\phi|_{\phi=\bar{\phi}}$. The shape of the corresponding IR is shown in Fig. 3 and can be explained with similar arguments as in Section 3.1. Again, Laplace Transform recovers exactly the FTF of Shreekrishna et al. [8, Eq. (24)].

For lean premixed flames the sensitivity S_{s_L} is positive and therefore the IR is positive. For rich mixtures, additional fuel leads to a decrease in the laminar flame speed and the IR is reversed.

3.3. Fluctuations of flame surface area

The third term on the right hand side of Eq. (1) stands for the contribution of flame surface area fluctuations to the IR of the heat release rate. This mechanism was already discussed by Blumenthal et al. [10], albeit only for the perturbations in velocity. Relevant time scales of restoration τ_r and convection τ_c were revealed, their impact on flame dynamics was discussed. In the present study, a similar approach is developed for the effects of equivalence ratio perturbations on flame shape and heat release rate. The similarity comes from the fact that the perturbed flame position ξ depends on V' and s'_L, as described in the right hand side of Eq. (3). The similarity is attributed to Eq. (3), where V' and s'_L act as source terms for the perturbed flame position ξ.

The first step is to compute ξ. Equation (3) for $\xi(X, t)$ can be formulated as an integral equation

$$\xi(X,t) = -\frac{1}{\bar{U}} \int_0^X s'_L\left(X', t - \frac{X - X'}{\bar{U}}\right) \mathrm{d}X' \,, \tag{10}$$

where laminar flame speed fluctuations caused by ϕ' are considered solely ($V' = 0$). The IR contribution is calculated as

$$h_A(t) = \frac{1}{\varepsilon}\frac{A'(t)}{\bar{A}} = \frac{2}{\varepsilon L_f^2 \tan\alpha} \int_0^{L_f} \xi(X,t)\, \mathrm{d}X \,. \tag{11}$$

In order to calculate the closed form IR, $\phi' = \bar{\phi}\varepsilon\delta\left(t - X/\bar{W}\right)$ is substituted in Eq. (10) and ξ is

Please cite this article as: A. Albayrak et al., An analytical model for the impulse response of laminar premixed flames to equivalence ratio perturbations, Proceedings of the Combustion Institute (2016), http://dx.doi.org/10.1016/j.proci.2016.06.002

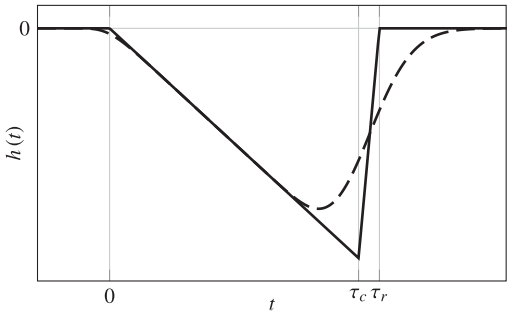

Fig. 5. Contribution of fluctuations of flame surface area to IR. Model without (——) and with dispersion (– –).

expressed as

$$\xi(X,t) = -\left.\frac{\mathrm{d}s_L}{\mathrm{d}\phi}\right|_{\phi=\bar{\phi}} \frac{\bar{\phi}\varepsilon\tau_r}{\tau_r-\tau_c}\left[H\left(t-\frac{X}{\bar{W}}\right) - H\left(t-\frac{X}{\bar{U}}\right)\right], \tag{12}$$

where $\tau_r = L_f/\bar{U}$ is the restorative time scale, which is defined as the time span for the hypothetical restoration line to travel from the base of the flame to its tip. ξ is illustrated with an intermediate flame shape perturbed with an impulse in Fig. 4.

The upper gray line ("Perturbation, $\bar{W}$") indicates the convection of impulsive perturbation and $\bar{W} = \bar{v}/\cos(\alpha)$ is the projection on $X-$direction. Since the mixture is assumed lean and the equivalence ratio perturbation is positive, the laminar flame speed perturbation is also positive. An increase in laminar flame speed overcomes the flow velocity normal to the flame surface and the flame propagates towards the base.

Starting from the anchoring point, where $\xi(0,t) = 0$, the restoration mechanism [10] re-establishes the original, unperturbed flame shape after the perturbation of equivalence ratio has passed. The lower gray line ("Restoration, $\bar{U}$") in Fig. 4 indicates up to which position the restoration process has progressed. This line travels with the speed $U = \bar{v}\cos(\alpha)$ in $X-$direction. The restoration line is upstream of the perturbation line, because of slower propagation speed.

By substituting ξ described in Eq. (12) into Eq. (11), the closed form IR is obtained

$$h_A(t) = -\frac{2S_{s_L}}{\tau_c(\tau_r-\tau_c)}\left[\frac{\tau_c}{\tau_r}\{R(t-\tau_r)-R(t)\} - \{R(t-\tau_c)-R(t)\}\right] \tag{13}$$

which is plotted in Fig. 5 with the solid line. Again the FTF given by Shreekrishna et al. [8, Eq. (26)] is exactly recovered by Laplace Transform.

The shape of the IR may be explained as follows: The perturbation ϕ' causes flame propagation towards the base and creates additional flame surface area indicated as "Overlap, A^+" in Fig. 4. At the same time, the restoration mechanism brings the flame to its old position and causes a deficit in flame surface area indicated as "Gap, A^-" in Fig. 4. Since the restoration process is slower, it acts at a position where the flame radius is larger than the one for the perturbation, thus the perturbed area is less than the steady area (negative IR in Fig. 5). As long as both processes act on the flame together, the deficit of flame surface area continuously increases. At late times $t > \tau_c$, when the perturbation has passed the flame, only the restorative mechanism acts to recover the original flame shape. The flame surface area deficit vanishes once the restoration line reaches the flame tip, which corresponds to the restorative time scale τ_r.

This section concludes with a comment on the study of Cho and Lieuwen [7], who derived time domain representations of flame dynamics by inverse Laplace transformation of frequency domain results. However, the IR was not recovered, because a generic form of perturbations was considered instead of an impulse perturbation. A full time domain analysis of the flame response to a generic perturbation is not straightforward and was indeed not attempted by Cho and Lieuwen [7]. Instead, their results are valid only in the low-frequency, quasi-steady limit.

4. Extended model with dispersion

In typical technical premixed combustion systems, the fuel is injected from a considerable distance upstream of the flame. This distance is important for the equivalence ratio perturbations because of dispersion due to molecular diffusion for a laminar flame. Generalization to turbulent dispersion is straightforward, but not discussed further here (refer to Polifke et al. [13], Lawn and Polifke [11], Schuermans et al. [12] and Bobusch et al. [14]). As the injection point moves further upstream, a wider Gaussian distribution instead of an impulse (Dirac function) arrives at the flame base and thus the impact on flame dynamics becomes weaker.

The model described in Section 2 and also previous models [7–9] employ an advection equation as described in Eq. (6). The impact of the species diffusion can be accounted by considering 1-D advection-diffusion equation with impulse perturbation at flame base $y = 0$, which reads

$$\frac{\partial\phi'}{\partial t} + \bar{v}\frac{\partial\phi'}{\partial y} = D\frac{\partial^2\phi'}{\partial y^2}\,, \tag{14}$$

where D is the averaged diffusion coefficient. The analytical solution reads

$$\phi'(x,y,t) = \bar{\phi}\varepsilon\sqrt{\frac{1}{\pi\tau_d t}}\exp\left[-\frac{1}{\tau_d t}\left(t-\frac{X}{\bar{W}}\right)^2\right], \tag{15}$$

Please cite this article as: A. Albayrak et al., An analytical model for the impulse response of laminar premixed flames to equivalence ratio perturbations, Proceedings of the Combustion Institute (2016), http://dx.doi.org/10.1016/j.proci.2016.06.002

where $\tau_d = 4D/\bar{v}^2$ is the diffusive time scale, which describes the strength of the diffusion. The solution is expressed in the flame aligned coordinate system.

The formalism developed in Section 3 can also be applied to the extended model. For heat of reaction contribution, Eq. (8) is integrated with the diffusive perturbation equation (15) instead of the impulse equation (7) (same for laminar flame speed contribution). The resulting IR contribution reads

$$h_{\Delta H}(t) = \frac{S_{\Delta H}}{\tau_c^2}\left\{\Re(t-\tau_c) - \Re(t) + \tau_c \mathrm{erf}\left(\frac{t}{\sqrt{\tau_d t}}\right)\right\}, \tag{16}$$

where $\Re(t, \tau)$ is the smoothed Ramp function defined as

$$\Re(t-\tau) = \sqrt{\frac{\tau_d t}{\pi}}\exp\left(-\frac{(t-\tau)^2}{\tau_d t}\right) + (t-\tau)\mathrm{erf}\left(\frac{t-\tau}{\sqrt{\tau_d t}}\right). \tag{17}$$

The contribution of laminar flame speed fluctuations is the same as Eq. (16), but $S_{\Delta H}$ is replaced with S_{s_L}.

For flame surface area contribution, the flame surface deviation ξ is determined by integrating equation (10) again with the diffusive perturbation. The contribution is then computed by integrating the flame surface deviation Eq. (11) as

$$h_A(t) = -\frac{S_{s_L}}{\tau_c(\tau_r - \tau_c)}\left[\frac{\tau_c}{\tau_r}\{\Re(t-\tau_r) - \Re(t)\} - \{\Re(t-\tau_c) - \Re(t)\}\right]. \tag{18}$$

The resulting IRs are plotted in Figs. 3 and 5 with dashed lines, for heat of reaction (same for laminar flame speed) and flame surface area, respectively.

The model can be extended for the cases, where the perturbation is imposed upstream of the flame base, say $y = -y_0$. The additional time lag for the perturbation to travel till the flame base $\tau_0 = y_0/\bar{v}$ can be accounted by change of variable of $t = t^* - \tau_0$ in Eqs. (15)–(18).

5. Validation against numerical simulation

A numerical simulation of a 2D axisymmetric conical flame is performed to validate the analytical model. Length and radius of the upstream flow duct are both 1 mm, the downstream radius of the computational domain is 6 mm in order to prevent confinement effects. A uniform mesh is constructed with a cell size of 0.02 mm. Slip and adiabatic wall boundary conditions are imposed to correspond with the analytical framework. A lean mixture of CH_4 and air ($\bar{\phi} = 0.8$) is used, the inflow velocity is $\bar{v} = 1$ m/s (Reynolds number 130) at a temperature of 293 K. A 2-step reduced chemistry is employed [15] in rhoReactingFoam (OpenFOAM solver), which is modified to assume Prandtl number of 0.7. The averaged molecular diffusivity was set to $D = 0.22 \times 10^{-4}\mathrm{m}^2/\mathrm{s}$, appropriate for CH_4 in air [16].

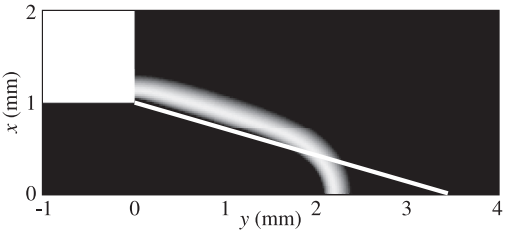

Fig. 6. Flame shapes: G-Equation model vs. numerical simulation with 2-step chemistry.

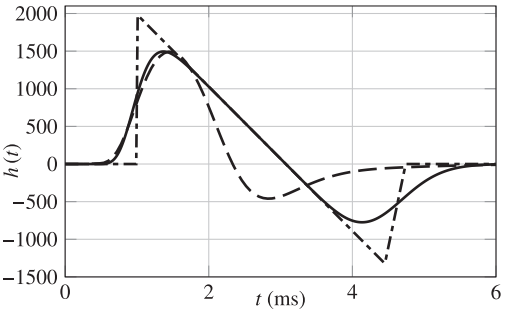

Fig. 7. Impulse response functions of conical laminar premixed flame. Analytical model without dispersion (– - –), with dispersion (——) and CFD results (– –).

Figure 6 compares the distribution of steady heat release rate from CFD against the analytical *G*-Equation flame. Close to the tip, curvature effects – which are not considered in *G*-Equation used – result in a comparatively shorter flame length of the CFD model.

Broadband equivalence ratio perturbations with an amplitude of $\varepsilon = \phi'/\bar{\phi} = 0.05$ are imposed at the inlet. The corresponding IR is determined via system identification (for details see [17]) and compared against the analytical model in Fig. 7. The latter includes all three contributions discussed above, see Fig. 1.

Including dispersion in the analytical model gives a "smeared out" response, in qualitative agreement with CFD. More than that, Fig. 7 shows very good quantitative agreement between CFD and the dispersive model for the early period $t <$ 2 ms.

At later times, the impulse response is negative before it decays to zero. This important feature, which is responsible for the excess gain of the FTF (see below) is reproduced qualitatively by both models based on the *G*-Equation. Nevertheless, it is apparent that at later times $t > 2$ ms quantitative

Please cite this article as: A. Albayrak et al., An analytical model for the impulse response of laminar premixed flames to equivalence ratio perturbations, Proceedings of the Combustion Institute (2016), http://dx.doi.org/10.1016/j.proci.2016.06.002

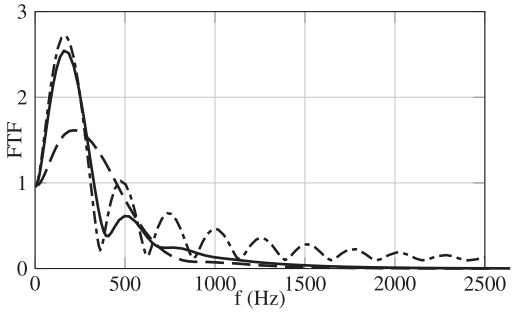

Fig. 8. Gain of FTF. Analytical model without dispersion (– – –), with dispersion (——) and CFD results (— —).

agreement with CFD deteriorates. This is due to the over-predicted flame length of the G-Equation model, resulting from the neglect of curvature effects. Note that the overall duration of the IR is related to the restorative time scale $\tau_r = L_f/\bar{U}$. Since the flame length L_f is over-predicted, the resulting IR is also more pronounced at late times.

Figure 8 compares the gain of the FTFs determined with the analytical model and the CFD simulation, respectively. Important qualitative features are reproduced by both analytical model formulations: the overall low pass filter behavior is observed, initial overshoot in gain is present, the low frequency limit (see Polifke and Lawn [18]) is correctly captured as unity.

The dash-dotted line indicates the FTF from the analytical model without dispersion. The model shows oscillatory behavior in the high frequency range, which is eliminated by dispersion (shown with solid line).

Both analytical and numerical results exhibit excess gain $|FTF| > 1$ at frequencies around 200 Hz. Excess gain results from constructive superposition of the positive and negative parts of the IR, as discussed by Huber and Polifke [19] and Blumenthal et al. [10]. The analysis in Section 3 has shown that the positive part of the IR results from fluctuations in heat of reaction and flame speed, while the negative part is due to the modulation of flame surface area. In the low frequency limit there is destructive superposition of these effects, which becomes constructive at intermediate frequencies, resulting in excess gain. Indeed, earlier models that did not take into account changes in flame surface area do not exhibit excess gain [13,20].

The intermediate frequency $f_{\max}$ where the gain attains its maximum can be roughly estimated as

$$f_{\max} \approx \frac{\pi}{2(t_{\max} - t_{\min})}, \tag{19}$$

where $t_{\max}$ and $t_{\min}$ are the times where the IR reaches maximal/minimal values. For the analytical model with dispersion, one estimates $f_{\max} \approx 200$ Hz, which agrees with the gain of the FTF shown in Fig. 8. For the CFD results, the negative part of the IR appears earlier and is less pronounced (see Fig. 6), thus excess gain occurs at higher frequencies and with reduced magnitude, as seen in Fig. 8.

6. Conclusion

The response of laminar premixed flame to equivalence ratio perturbations was studied analytically by determining the IR for heat release rate. In the framework of the G-Equation contributions of heat of reaction, laminar flame speed and flame surface area were taken into consideration. Two relevant time scales were identified, i.e. a convective time scale τ_c and a restorative time scale τ_r. The transport of equivalence ratio perturbations is related to τ_c, while the propagation of flame shape perturbations along the flame is related to τ_r. The contributions of heat of reaction and laminar flame speed are governed only by τ_c, since the convective perturbations of equivalence ratio causes local changes at the flame surface. The contribution of flame surface area is controlled by both τ_c and τ_r due to the restoration mechanism. Complete agreement with flame transfer functions calculated by Shreekrishna et al. [8] was established by Laplace transformation of IRs.

An extension to the model was proposed in order to account for the dispersion due to molecular diffusion. The dispersive model adds one more time scale τ_d regarding the strength of the dispersion. As the location of the perturbation moves further away from the flame, its impact on the flame dynamics becomes weaker [13].

Analytical models were compared against numerical simulation by examining the respective IRs and FTFs. Quantitative agreement was not achieved, since the analytical G-Equation model used in this study neglects curvature effects and thus over-predicts the flame length. Nevertheless, very satisfactory qualitative agreement with respect to the shape of the IR and the relevant time scales was observed. Overall, the model with dispersion showed significantly better agreement than the model without dispersion.

The analysis in the paper shows that excess gain in the flame response to equivalence ratio fluctuations results from constructive superposition of the effects of fluctuations in heat of reaction and flame speed on the one hand, and the effects of modulation of flame shape on the other.

Acknowledgments

The presented work is part of the Marie Curie Initial Training Network *Thermo-acoustic and aero-acoustic nonlinearities in green combustors with orifice structures* (TANGO). We gratefully acknowledge the financial support from the

Please cite this article as: A. Albayrak et al., An analytical model for the impulse response of laminar premixed flames to equivalence ratio perturbations, Proceedings of the Combustion Institute (2016), http://dx.doi.org/10.1016/j.proci.2016.06.002

European Commission under call FP7-PEOPLE-ITN-2012. Financial support for A. Ulhaq was provided by higher education commission (HEC) of Pakistan. Financial support for R. S. Blumenthal was provided by Technische Universität Müchen, Institute for Advanced Study, funded by the German Excellence Initiative, and German Research Foundation DFG, project PO 710/12-1.

References

[1] T.C. Lieuwen, *Unsteady Combustor Physics*, Cambridge University Press, 2012.
[2] L. Boyer, J. Quinard, *Combust. Flame* 82 (1990) 51–65.
[3] A. Fleifil, A.M. Annaswamy, Z.A. Ghoneim, A.F. Ghoniem, *Combust. Flame* 106 (1996) 487–510.
[4] T. Schuller, D. Durox, S. Candel, *Combust. Flame* 134 (1) (2003) 21–34.
[5] A.R. Kerstein, W.T. Ashurst, F.A. Williams, *Phys. Rev. A* 37 (1988) 2728.
[6] A. Dowling, S. Hubbard, *Proc. Inst. Mech. Eng., Part A J. Power Energy* 214 (4) (2000) 317–332.
[7] J.H. Cho, T. Lieuwen, *Combust. Flame* 140 (1) (2005) 116–129.
[8] Shreekrishna, S. Hemchandra, T. Lieuwen, *Combust. Theor. Model.* 14 (5) (2010) 681–714.
[9] S. Hemchandra, in: ASME Turbo Expo: Turbine Technical Conference and Exposition, GT2011-45590, American Society of Mechanical Engineers, 2011, pp. 567–578.
[10] R.S. Blumenthal, P. Subramanian, R. Sujith, W. Polifke, *Combust. Flame* 160 (7) (2013) 1215–1224.
[11] C.J. Lawn, W. Polifke, *Combust. Sci. Technol.* 176 (2004) 1359–1390.
[12] B. Schuermans, V. Bellucci, F. Guethe, F. Meili, P. Flohr, O. Paschereit, in: International Gas Turbine and Aeroengine Congress & Exposition, GT2004-53831, 2004.
[13] W. Polifke, J. Kopitz, A. Serbanovic, in: 7th AIAA/CEAS Aeroacoustics Conference, AIAA 2001–2104, 2001. Maastricht, The Netherlands
[14] B.C. Bobusch, B. Ćosić, J.P. Moeck, C. Oliver Paschereit, in: Journal of Engineering for Gas Turbines and Power, vol. 136, 2013, p. 021506, doi:10.1115/1.4025375.
[15] J. Bibrzycki, T. Poinsot, A. Zajdel, *Archivum Combustionis,* A. Teodorczyk, Varsovie, Pologne 30 (2010) 287–296.
[16] M. Cowie, H. Watts, *Can. J. Chem.* 49 (1) (1971) 74–77.
[17] W. Polifke, *Ann. Nuclear Energy* 67C (2014) 109–128, doi:10.1016/j.anucene.2013.10.037.
[18] W. Polifke, C.J. Lawn, *Combust. Flame* 151 (3) (2007) 437–451, doi:10.1016/j.combustflame.2007.07.005.
[19] A. Huber, W. Polifke, *Int. J. Spray Combust. Dyn.* 1 (2) (2009) 199–228.
[20] J.F. v Kampen, J.B.W. Kok, T.H. van der Meer, in: 12th International Congress on Sound and Vibration (ICSV12), IIAV, Lisbon, Portugal, July 11-14 2005.

Please cite this article as: A. Albayrak et al., An analytical model for the impulse response of laminar premixed flames to equivalence ratio perturbations, Proceedings of the Combustion Institute (2016), http://dx.doi.org/10.1016/j.proci.2016.06.002